

Redesigning a flexural joint for metal-based additive manufacturing

Original

Redesigning a flexural joint for metal-based additive manufacturing / Ercolini, Edoardo; Calignano, Flaviana; Galati, Manuela; Viccica, Marco; Iuliano, Luca. - ELETTRONICO. - 100:(2021), pp. 469-475. ((Intervento presentato al convegno 31st CIRP Design Conference 2021 tenutosi a Twente nel 19 May 2021 - 21 May 2021 [10.1016/j.procir.2021.05.106].

Availability:

This version is available at: 11583/2911352 since: 2021-07-07T08:24:00Z

Publisher:

Elsevier

Published

DOI:10.1016/j.procir.2021.05.106

Terms of use:

openAccess

This article is made available under terms and conditions as specified in the corresponding bibliographic description in the repository

Publisher copyright

Elsevier postprint/Author's Accepted Manuscript

© 2021. This manuscript version is made available under the CC-BY-NC-ND 4.0 license
<http://creativecommons.org/licenses/by-nc-nd/4.0/>. The final authenticated version is available online at:
<http://dx.doi.org/10.1016/j.procir.2021.05.106>

(Article begins on next page)

31st CIRP Design Conference 2021 (CIRP Design 2021)

Redesigning a flexural joint for metal-based additive manufacturing

Edoardo Ercolini^a, Flaviana Calignano^a, Manuela Galati^a, Marco Viccica^{a,*}, Luca Iuliano^a

^a*Integrated Additive Manufacturing Center (IAM) Politecnico di Torino, Department of Management and Production Engineering (DIGEP), Torino 10129, Italy; luca.iuliano@polito.it*

* Corresponding author. Tel.: +39-011-090-7280. E-mail address: marco.viccica@polito.it

Abstract

Traditional rigid mechanisms exhibit problems such as assembly difficulties, friction and lubrication. Flexure-based compliant mechanisms, instead, are monolithic and gain their mobility thanks to proper design and material deflection. Designing and producing a compliant mechanism accurately and conveniently is crucial. Thanks to its capabilities, additive manufacturing (AM) approach can provide optimal design and production and open the way to new, unexploited performances.

This study investigates the redesign of a traditional cantilevered pivot. The redesign considers the performance improvements by exploiting the advantages of the AM based on laser powder bed fusion (L-PBF).

The maximum tensile and compressive loads of the redesigned joint were identified. The structure was optimised by considering the most critical geometrical parameters in terms of mechanical performance. The geometrical factors comply with the design rules for L-PBF process, to maximise the dimensional and surface accuracies. The new approach to the flexural joint design presented in this paper provided higher mobility if compared with the traditional approach. Therefore, this study makes a major contribution to research on the production of precision alignment mechanisms and scientific instruments.

© 2021 The Authors. Published by Elsevier Ltd.

This is an open access article under the CC BY-NC-ND license (<https://creativecommons.org/licenses/by-nc-nd/4.0>)

Peer-review under responsibility of the scientific committee of the 31st CIRP Design Conference 2021.

Keywords: Structural Analysis; Design for Additive Manufacturing; AlSi10Mg; Metal; Powder Bed Fusion

1. Introduction

Flexible joints, also known as flexible pivots, are compliant mechanisms, i.e. systems that move partially or completely due to the deformability of some of their parts, rather than the relative motion of rigid parts [1].

The advantages of using flexible pivots when compared to traditional rotation joints are numerous [2,3]. The movement of a flexible joint is guaranteed by its elastic deformation, without backlashes. Friction is absent since there are no rotating elements or sliding couples, thereby wear is limited to the material fatigue. Thanks to the absence of parts that move relatively to each other, no lubrication is required, thus flexible joints are ideal for applications that require high levels of cleanliness. Nevertheless, compared to the traditional, some flexible joints have low stiffness in non-deformation directions [4].

Typically, flexible pivots consist of rigid and flexible parts. The rigid part, usually known as sleeves, allow the coupling to the working system, whereas the flexible parts are responsible for the pivot movement itself. From a production standpoint, conventional flexible joints can be produced from a monolithic block or assembling different parts.

The most used production techniques to produce monolithic flexural joint are CNC 3-axis milling and Wire Electro-Discharge Machining (WEDM) [5]. The simplest monolithic flexible joint is the flexure hinge which is produced by CNC and is used in micro-nano positioning systems [6–12].

Owing to the manufacturing limitation, most of the flexible pivots are assembled: the flexible elements are welded/brazed on the sleeve, e.g. the cantilevered pivot first introduced in [13,14], or connected to it via screws/pins, e.g. the cross axis pivot studied in [15]. In this case, the performances of the joint are strongly affected by assembly and manufacturing errors.

Additive Manufacturing (AM) techniques could tackle the challenge of reducing the above-mentioned errors while also introducing numerous advantages. Components are fabricated in a layer-by-layer manner, and therefore, even joints with complex shape can be produced as a single part. As a result, precision monolithic joints can be produced easily and keeping a high-performance degree. In addition, AM is suitable for low production volumes, which are typical of flexible joint applications.

A review of the literature revealed that there are both polymeric and metallic AM applications to flexible systems. Polymeric components with flexible kinematic chains have been designed for the medical field for endoscopic instruments [16–19], for the soft robotic device [20–22], and for the development of joints for smart materials used with 4D printing [23]. However, polymeric components suffer from problems such as low stiffness, creep deformation, short life cycle, which make them unsuited for fields such as aerospace [24]. To date, there are only a few studies about metal flexible pivots fabricated by AM. Merriam et al. [25,26] presented a titanium aiming system composed of a “split tube” flexure and cross-axis pivots manufactured via electron beam melting (EBM). The EBM technique was also used by Merriam and Howell in [27], where lattice structures were used to reduce the weight of a cross-axis pivot structure. The lattice structures were also involved in reducing the joint stiffness, which allowed larger strokes. Riede et al. [28] presented a flexible joint designed for production via laser metal deposition (LMD). A stroke of $\pm 30^\circ$ was obtained during testing. However, the joint required finishing operations using WEDM. In Wei et al. [24], a simple flexible AISI 316L hinge made via laser powder bed fusion (L-PBF) was presented. Despite R_a values, referred to as the arithmetic mean roughness, by machining are much lower [29], the results showed that L-PBF guarantees an adequate surface finishing ($R_a = 3 \div 8 \mu\text{m}$ [30,31]) to make the flexure mechanism suitable for precise positioning. Because of that, this technique appears to be the most suitable among the AM to produce high-performance flexural joints with high dimensional and geometrical accuracies with respect to other AM techniques for metals [32].

In L-PBF, a laser beam is used to melt, according to the processed data, selected areas of a metallic powder bed [33] and the part is built layer-by-layer. The control and the shape of the beam are fine and precise and allow to obtain part with small details fabricated with high precision and dimensional accuracy ($40 \div 70 \mu\text{m}$) [34–36].

In the present work, a conventional flexible assembled pivot is redesigned to be fabricated using the L-PBF production technique. The study makes evident the need to exploit the full potential of L-PBF and overcome the most common design problems in designing high-performance flexural joints. Initially, a traditional redesign approach for AM is adopted. Therefore, the original joint is considered as a single part and then adapted to improve its feasibility by the L-PBF process. The performances of this redesigned joint are compared with the original design. From this comparison, the joint is newly designed.

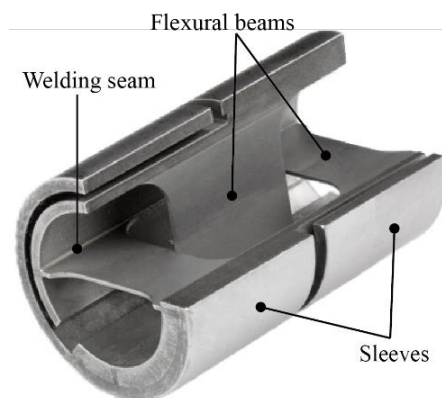


Fig. 1. Section-view of a generic cantilevered pivot by Riverhawk’s Flexural Pivot [37].

In this case, the original design is completely abandoned toward a perfect match between manufacturing feasibility and structural performances.

2. Case Study

The case study concerns the redesign of a cantilevered pivot. The original design consists of two cylindrical sleeves connected by two thin flat flexures perpendicular to each other. Each sleeve has an annular section that projects into the other without touching it [13].

The flexible elements are jointed on the sleeves by brazing or electro-welding. The selected geometry is commercial [37,38]. The rotation angle of the selected joint is ± 3.7 degrees. An example of internal cantilevered pivot geometry is shown in Fig. 1.

2.1. Original geometry, simulations and geometry optimisation

As discussed above, the production by AM eliminates the assembly phase. Therefore, the first step was to redesign the cantilevered pivot as a single piece. The first design modification used fillets to reduce thermal stress concentration of the sharp edges, and the flat flexures (Fig. 2) [39].

Therefore, the monolithic pivot was modelled by finite elements, and the load conditions were simulated using ANSYS 16.0. The AM aluminum alloy, AlSi10Mg, was set as material, whose related properties were extracted from the datasheet of the manufacturer of the powder used in this work [40]. The load cases were a) a tensile radial load, b) compression radial load, and c) rotation. The rotation load case means the rotation of the unconstrained sleeve around the axis of the pivot. This load condition is accomplished by fixing one sleeve in a circular hole while the second sleeve is subjected to the load. These constraints are typical for these types of pivots [41]. The simulations aimed to identify the tensile and compressive load and the rotation of the joint for which the joint reach the yield stress (230 MPa). The safety coefficient of the structure was therefore set equal to 1.

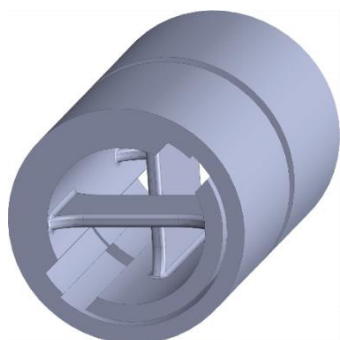


Fig. 2. Redesigned joint.

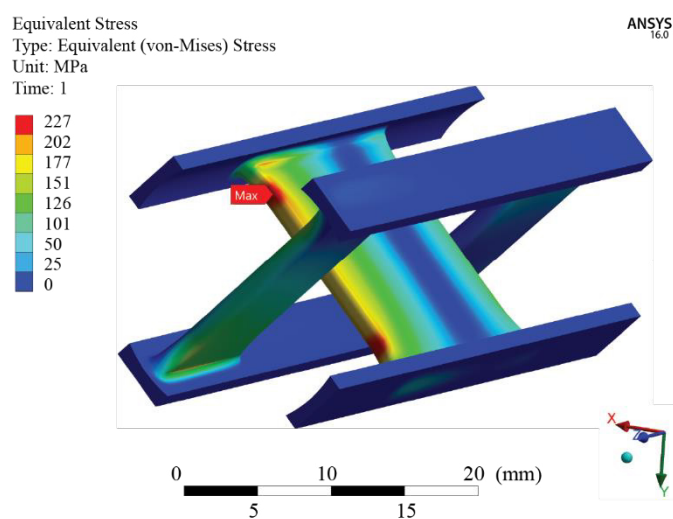


Fig. 3. Equivalent Von Mises stress under tensile load.

Each load condition and corresponding maximum equivalent Von Mises stress obtained from the simulations are shown in Table 1.

Table 1. Simulation results.

Load Case	Maximum load / rotation	Maximum equivalent stress [MPa]
Tensile	1375 N	227
Compression	1375 N	230
Rotation	3.2 °	228

As an example, Fig. 3 shows the maximum stress evolution corresponding to the maximum tensile radial load supported by the structure. Only flexible elements were simulated as the sleeves do not affect the pivot performance. The rotation values proved to be consistent with the literature [38]. However, the areas of concentrated stresses can be detrimental to the performance of the flexible elements and, therefore, the geometry modifications were necessary. The geometric parameters considered to reduce the tension are shown in Fig. 4. To maintain the maximum flexibility of the element, the thickness of the flexible elements (s) was set equal to the minimum, which can be manufactured by L-PBF. Therefore, s

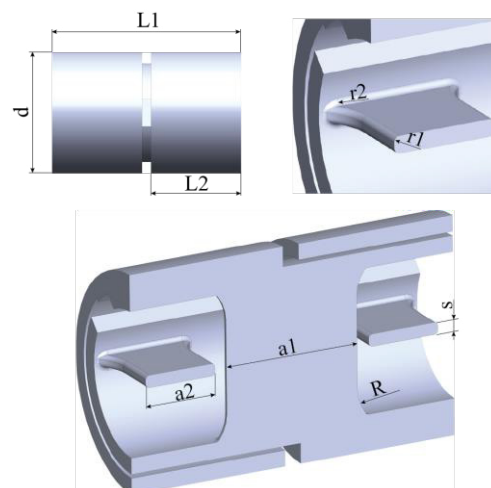


Fig. 4. Geometric parameters.

was set equal to 1.5 mm. A sensitivity analysis was performed on the parameters $a1$ and $a2$. It was found that an increase of the width of the flexible element $a1$ and a corresponding reduction of the width $a2$ involves a significant decrease of the equivalent stress. Besides, as the R-value increases so the safety coefficient increases.

These geometry modifications reduced the maximum equivalent Von Mises stress (σ_{max}) from 230 MPa to 139 MPa under the same applied load (1375 N). The values of geometric parameters are shown in Table 2.

Table 2. Geometric parameters before and after geometry optimisation.

	r1 [mm]	r2 [mm]	R [mm]	s [mm]	a1 [mm]	a2 [mm]	σ_{max} [MPa]
Original design	0.5	0.5	5	1.5	17	9	230
Optimised design	0.5	0.5	7	1.5	23	6	139

The geometry has been further modified by topology optimising the material in the central area of the flexure, in which the stresses are close to zero (Fig. 3) [42]. The material was removed by keeping constant the admissible equivalent stress (139 MPa). The final optimised geometry is shown in Fig. 5a.

At his point, the joint was then analysed to determine the maximum load that leads to a safety factor equal to 1. The obtained results of both tensile and compression were 2250 N and 2225 N, respectively. The maximum rotation that can be performed before yielding is 3.4°, slightly lower than the original design.

2.2. Design for L-PBF

Owing to the performance achieved, the geometry of the component has been further optimised to improve its feasibility by L-PBF. The approach proposed by Galati et al. [43] has been adopted. The main design drive is the accuracy of the sleeves

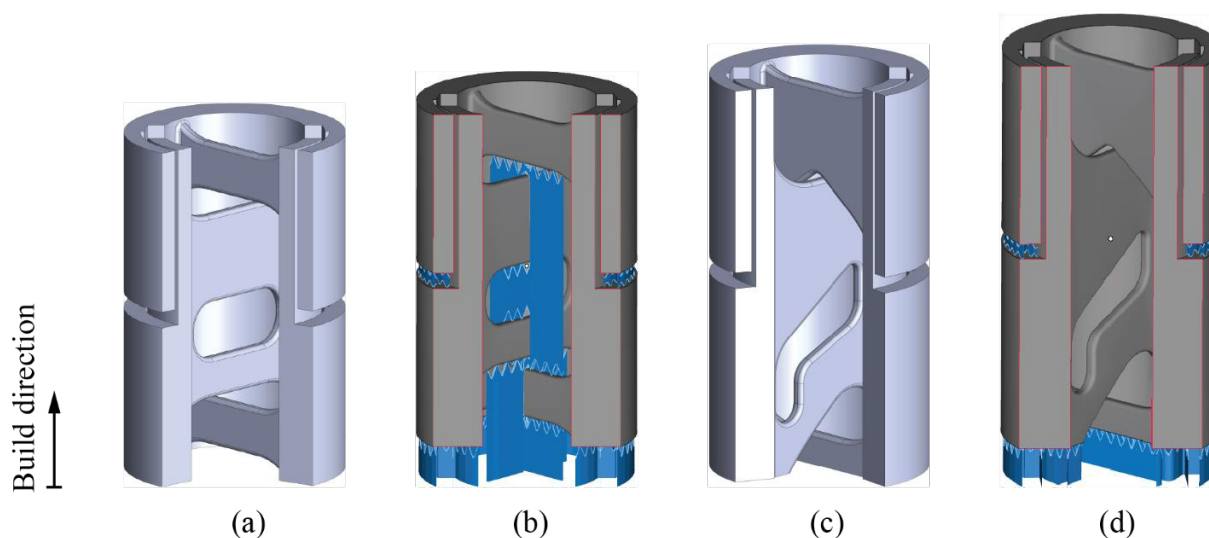


Fig. 5. Cross-section of the optimised design (a) and build orientation of the pivot with the support structure (in blue) (b). Cross-section of the component optimised for L-PBF production (c), and its build orientation with support structure (in blue) (d).

which must be guaranteed in the coupling area. Therefore, the build orientation of the component was fixed to be parallel to the sleeve axis. This orientation also involves the use of a low number of support structures. However, the presence of external sleeves and the small size of the joint hinder the access to the inside of the structure, making it impossible to remove any support. The joint surfaces have therefore been modified into self-supported surfaces. A minimum angle α equals 35° was chosen between the overhanging surfaces and the build platform [44].

The result of the redesign obtained by following the described previous adjustments is shown in Fig. 5c.

Compared to the previous (Fig. 5a), the new design shows fewer supports, easily removed.

The redesigned pivot was numerically verified under the three load cases reported in paragraph 2.1. The results showed that the maximum rotation value reached before yielding was 2.4° , which is lower than the previous design. This reduction may be attributed to narrow fittings on the top and at centre of the flexible elements, which causes a stress concentration effect. Furthermore, the widths of the flexible elements exceed the widths of the previously obtained geometry, making the redesigned pivot stiffer than the previous.

This result clearly shows that, with a proper design, it is possible to produce flexural joint by L-PBF. However, the geometry modifications required to make the product feasible by this technology constrained the performance of the component.

3. Cantilever pivot for L-PBF

A novel structure was designed while preserving only the functionality and the coupling surfaces of the original pivot. The main objective has been to enhance the structural performance of the original joint by achieving a minimum rotation of at least 5° . Rotation alone was considered as this

pivot is mainly used in place of bearings due to its non-friction properties in precision alignment mechanisms and scientific instruments. In these instruments, the degree of rotation is mainly considered. Small-angle generators are widely used in dimensional metrology to calibrate, for example, high-resolution electronic autocollimators. Nowadays, these requirements can be easily achieved by using microactuators, so-called piezo nano-positioner pushers and flexural mechanisms.

The maximum envelope was fixed to be equal to the original structure envelope, whereas the coupling elements of the structure were designed with two parallel rings. As before, the build direction was set parallel to the axis of the rings to ensure the right dimensional and geometrical accuracy [32,35]. The two rings are connected with a series of helix wires with a twisted profile (Fig. 6). The use of helix profiles and ring structures allowed the maximisation of the component's lightening. From a L-PBF production point of view, the internal emptiness of the structure enables greater freedom access during the support removal. Additionally, a proper torsion of the helicoidal profile ensures that the helixes are self-supporting. Therefore, supports are required only to anchor the bottom ring to the build platform and to support the construction of the upper ring.

A sensitivity analysis has been performed to understand the performance of the new joint. The most influential parameters are the wire diameter of the helix and its torsion. A larger helix wire diameter corresponds to greater stiffness and, therefore, a lower rotation capacity of the helix.

To meet the needs of both manufacturing constraints and stiffness of the pivot, a minimum diameter value of 2 mm was chosen for the wire. As concerns the profile torsion, it was found out that a greater twist of the helixes corresponds to a greater rotation of the joint.

The obtained results are shown in Table 2. The maximum rotation and the corresponding maximum equivalent Von

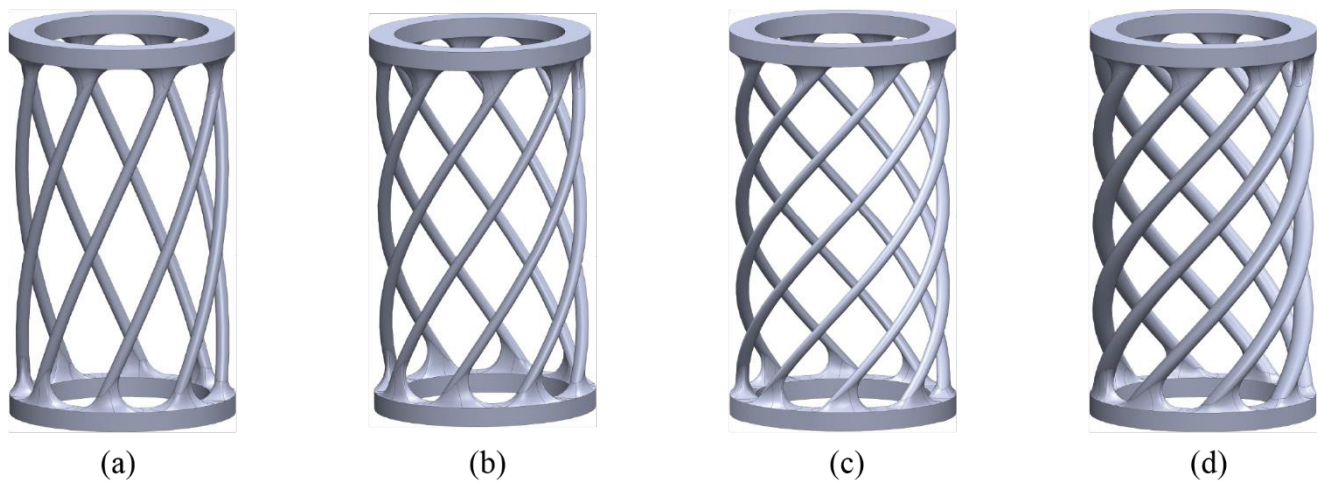


Fig. 6. Alternative configurations. Geometric parameters are indicated in Table 3.

Mises stress values refer to a safety coefficient of 1. The simulations were performed under the same conditions as the previous design.

Table 3. Results for different geometry configurations.

Geometry	Helix wire diameter [mm]	Profile torsion [°]	Maximum rotation [°]	Maximum equivalent stress [MPa]
(a)	2	90	5.3	227
(b)	2	135	6.4	229
(c)	2	180	7.4	230
(d)	3	180	5.4	229

All the new designs satisfied the minimum required rotation of 5°. Higher-profile torsion (Fig. 6c) leads to a maximum rotation equal to 7.4° in case (c). The profile torsion over 180° has not been investigated because the self-supporting requirement is violated. The diameter increase reduces the overall rotation value, as shown for the geometry (d) in Fig. 6.

The increase of torsional performance, by reducing the pivot structural material, implied decreasing admissible radial load.

4. Conclusion

In literature, the AM design approach for flexible joints lacks investigation. This work illustrated how the design of compliant assembled mechanisms could benefit from the AM capability, in particular for L-PBF based production. Among the flexural joints, a cantilever pivot was analysed.

The pivot was firstly redesigned, adapting the traditional geometry to the L-PBF production. The main advantage was the removal of the assembly operations that affected the performance of the original design. However, the modified design showed poor performance compared to the original. In light of this result, a novel geometry was developed. The component design was fully disrupted by embedding a series of helix brackets between the coupling parts of the pivot. The results showed enhanced mechanical performances with

respect to the traditional design. The L-PBF technique made it possible to build the cantilever pivot as a monolithic part (from four components to one) and remove any assembly operation. The proposed innovative structure (18 g AM aluminum alloy) is 40% lighter than the original structure (30 g cast aluminum alloy). For the geometry with lower profile torsion, the obtained rotation is 2.1° and 2.9° higher than the original design (3.2°) and the redesigned pivot for L-PBF (2.4°), respectively.

These results prove that the benefits of the AM capabilities can be fully exploited only if a paradigm change is adopted: simply redesigning or adjusting the geometry for production is insufficient. This case study shows the potential of exploiting AM in designing new flexural joints and it adds to the rapidly expanding field of the precision mechanical components production.

References

- [1] Yang Y, Di W, Xubin S, Chen Y. Design and rapid fabrication of non-assembly mechanisms. Proc. 2010 Int. Conf. Manuf. Autom. ICMA 2010, vol. 1, IEEE; 2010, p. 61–3. <https://doi.org/10.1109/ICMA.2010.2>.
- [2] Howell LL, Magleby SP, Olsen BM. Handbook of Compliant Mechanisms. Chichester: 2013.
- [3] Trease BP, Moon YM, Kota S. Design of large-displacement compliant joints. J Mech Des Trans ASME 2005;127:788–98. <https://doi.org/10.1115/1.1900149>.
- [4] Wiersma DH, Boer SE, Aarts RGKM, Brouwer DM. Design and performance optimization of large stroke spatial flexures. J Comput Nonlinear Dyn 2014;9. <https://doi.org/10.1115/1.4025669>.
- [5] Henein S, Spanoudakis P, Droz S, Myklebust LI, Onillon E. Flexure pivot for aerospace mechanisms. Eur Sp Agency, (Special Publ ESA SP 2003:285–8).
- [6] Bhagat U, Shirinzadeh B, Clark L, Chea P, Qin Y. Design and analysis of a novel flexure-based 3-DOF mechanism. Mech Mach Theory 2014;74:173–87.
- [7] Yang R, Jouaneh M, Schweizer R. Design and characterization of a low-profile micropositioning stage. Precis Eng 1996;18:20–9.

- [https://doi.org/10.1016/0141-6359\(95\)00032-1](https://doi.org/10.1016/0141-6359(95)00032-1).
- [8] Tian Y, Shirinzadeh B, Zhang D. Design and dynamics of a 3-DOF flexure-based parallel mechanism for micro/nano manipulation. *Microelectron Eng* 2010;87:230–41. <https://doi.org/10.1016/j.mee.2009.08.001>.
- [9] Zhang X, Xu Q. Design of a new flexure-based XYZ parallel nanopositioning stage. 2015 IEEE Int Conf Robot Biomimetics, IEEE-ROBIO 2015 2015:1962–6. <https://doi.org/10.1109/ROBIO.2015.7419060>.
- [10] Liang Q, Zhang D, Chi Z, Song Q, Ge Y, Ge Y. Six-DOF micro-manipulator based on compliant parallel mechanism with integrated force sensor. *Robot Comput Integr Manuf* 2011;27:124–34. <https://doi.org/10.1016/j.rcim.2010.06.018>.
- [11] Tian Y, Shirinzadeh B, Zhang D. A flexure-based five-bar mechanism for micro/nano manipulation. *Sensors Actuators, A Phys* 2009;153:96–104. <https://doi.org/10.1016/j.sna.2009.04.022>.
- [12] Yi BJ, Chung GB, Na HY, Kim WK, Suh IH. Design and experiment of a 3-DOF parallel micromechanism utilizing flexure hinges. *IEEE Trans Robot Autom* 2003;19:604–12. <https://doi.org/10.1109/TRA.2003.814511>.
- [13] Troeger H. Considerations in the application of flexural pivots. *Autom Control Data Syst Eng* 1962;17.
- [14] Seelig FA. Flexural Pivots for Space Applications. *Proc. 3rd Aerosp. Mech. Symp. Held Jet Propuls. Lab. Pasadena, Calif., 1968*, p. 9–18.
- [15] Folkersma KGP, Boer SE, Brouwer DM, Herder JL, Soemers HMJR. A 2-DOF large stroke flexure based positioning mechanism. *Proc. ASME Des. Eng. Tech. Conf.*, vol. 4, 2012, p. 221–8. <https://doi.org/10.1115/DETC2012-70377>.
- [16] Roppenecker DB, Traeger MF, Gumprecht JDJ, Lueth TC. How to design and create a cardan shaft for a single port robot by selective laser sintering. *ASME Int Mech Eng Congr Expo Proc* 2012;3:49–58. <https://doi.org/10.1115/IMECE2012-87654>.
- [17] Roppenecker DB, Pfaff A, Coy JA, Lueth TC. Multi arm snake-like robot kinematics. *IEEE Int Conf Intell Robot Syst* 2013:5040–5. <https://doi.org/10.1109/IROS.2013.6697085>.
- [18] Krieger YS, Roppenecker DB, Stolzenburg JU, Lueth TC. First step towards an automated designed Multi-Arm Snake-Like Robot for minimally invasive surgery. *Proc IEEE RAS EMBS Int Conf Biomed Robot Biomechatronics* 2016;2016-July:407–12. <https://doi.org/10.1109/BIOROB.2016.7523661>.
- [19] Coemert S, Traeger MF, Graf EC, Lueth TC. Suitability Evaluation of various Manufacturing Technologies for the Development of Surgical Snake-like Manipulators from Metals Based on Flexure Hinges. *Procedia CIRP* 2017;65:1–6. <https://doi.org/10.1016/j.procir.2017.03.108>.
- [20] Mutlu R, Alici G, Li W. A Soft Mechatronic Microstage Mechanism Based on Electroactive Polymer Actuators. *IEEE/ASME Trans Mechatronics* 2016;21:1467–78. <https://doi.org/10.1109/TMECH.2015.2502597>.
- [21] Mutlu R, Alici G, Li W. Three-Dimensional Kinematic Modeling of Helix-Forming Lamina-Emergent Soft Smart Actuators Based on Electroactive Polymers. *IEEE Trans Syst Man, Cybern Syst* 2017;47:2562–73. <https://doi.org/10.1109/TSMC.2016.2523940>.
- [22] Al-Rubaia M, Pinto T, Qian C, Tan X. Soft Actuators with Stiffness and Shape Modulation Using 3D-Printed Conductive Poly(lactic Acid) Material. *Soft Robot* 2019;6:318–32. <https://doi.org/10.1089/soro.2018.0056>.
- [23] Jeong HY, An SC, Seo IC, Lee E, Ha S, Kim N, et al. 3D printing of twisting and rotational bistable structures with tuning elements. *Sci Rep* 2019;9:1–9. <https://doi.org/10.1038/s41598-018-36936-6>.
- [24] Wei H, Wang L, Niu X, Deng Y, Zhang Y, Cheng J. Stiffness characteristics of a laser beam melted (LBM) additive-manufactured flexure mechanism. *Procedia CIRP* 2018;78:144–8. <https://doi.org/10.1016/j.procir.2018.09.051>.
- [25] Merriam EG, Jones JE, Magleby SP, Howell LL. Monolithic 2 DOF fully compliant space pointing mechanism. *Mech Sci* 2013;4:381–90. <https://doi.org/10.5194/ms-4-381-2013>.
- [26] Merriam EG, Jones JE, Howell LL. Design of 3D-Printed Titanium Compliant Mechanisms. *Proc. 42nd Aerosp. Mech. Symp.*, 2014, p. 169–74.
- [27] Merriam EG, Howell LL. Lattice flexures: Geometries for stiffness reduction of blade flexures. *Precis Eng* 2016;45:160–7. <https://doi.org/10.1016/j.precisioneng.2016.02.007>.
- [28] Riede M, Knoll M, Wilsnack C, Gruber S, Cubillo AA, Melzer C, et al. Material characterization of AISI 316L flexure pivot bearings fabricated by additive manufacturing. *Materials (Basel)* 2019;12. <https://doi.org/10.3390/ma12152426>.
- [29] Luo HP, Zhang B, Zhou ZX. A rotary flexural bearing for micromanufacturing. *CIRP Ann - Manuf Technol* 2008;57:179–82. <https://doi.org/10.1016/j.cirp.2008.03.033>.
- [30] BHASKAR REDDY, REDDY D, REDDY E. Experimental Investigations on Mrr and Surface Roughness of En 19 & Ss 420 Steels in Wire-Edm Using Taguchi Method. *Int J Eng Sci Technol* 2012;4:4603–14.
- [31] Kiener L, Saudan H, Cosandier F, Perruchoud G, Spanoudakis P, Rouvinet J. Additive manufacturing: Innovative concept of compliant mechanisms. *Proc 20th Int Conf Eur Soc Precis Eng Nanotechnology, EUSPEN 2020* 2020:137–40. <https://doi.org/10.1117/12.2560906>.
- [32] Minetola P, Galati M, Calignano F, Iuliano L, Rizza G, Fontana L. Comparison of dimensional tolerance grades for metal AM processes. *Procedia CIRP*, 2020. <https://doi.org/10.1016/j.procir.2020.05.069>.
- [33] Calignano F, Manfredi D, Ambrosio EP, Biamino S, Lombardi M, Atzeni E, et al. Overview on additive manufacturing technologies. *Proc IEEE* 2017;105:593–612. <https://doi.org/10.1109/JPROC.2016.2625098>.
- [34] Calignano F, Cattano G, Manfredi D. Manufacturing of thin wall structures in AlSi10Mg alloy by laser powder bed fusion through process parameters. *J Mater Process Technol* 2018;255:773–83.
- [35] Calignano F, Iuliano L, Galati M, Minetola P, Marchiandi G. Accuracy of down-facing surfaces in complex internal channels produced by laser powder bed fusion (L-PBF). *Procedia CIRP* 2020;88:423–6. <https://doi.org/10.1016/j.procir.2020.05.073>.
- [36] Calignano F, Galati M, Iuliano L. A metal powder bed fusion process in industry: Qualification considerations. *Machines* 2019;7:72.
- [37] Riverhawk's Flexural Pivot. *Flexural Pivot Catalog* 2017:1–2. <https://flexpivots.com/flexural-pivot-products/cantilevered-single-ended-pivot-bearings/> (accessed November 1, 2020).
- [38] C-Flex Bearing Co. Inc. *C-Flex Product Brochure* 2015:1–24. <https://c-flex.com> (accessed May 1, 2020).
- [39] Kranz J, Herzog D, Emmelmann C. Design guidelines for laser additive manufacturing of lightweight structures in TiAl6V4. *J Laser Appl* 2015. <https://doi.org/10.2351/1.4885235>.
- [40] EOS Material datasheet for Aluminium AlSi10Mg 2014.
- [41] C-Flex Bearing Co. Inc. *Pivot bearing design guide* 2015:1–20.

<https://c-flex.com> (accessed May 1, 2020).

- [42] Salmi A, Calignano F, Galati M, Atzeni E. An integrated design methodology for components produced by laser powder bed fusion (L-PBF) process. *Virtual Phys Prototyp* 2018;13:191–202.
- [43] Galati M, Calignano F, Viccica M, Iuliano L. Additive Manufacturing Redesigning of Metallic Parts for High Precision Machines. *Crystals* 2020;10:161.
- [44] Calignano F. Design optimization of supports for overhanging structures in aluminum and titanium alloys by selective laser melting. *Mater Des* 2014. <https://doi.org/10.1016/j.matdes.2014.07.043>.